유한요소해석에 의한 공구마모의 파괴역학적 모델링 연구

서욱환† · 이영섭*
한라대학교 기계자동차공학부 · *강원대학교 대학원 기계메카트로닉스공학과
(2004. 3. 2. 접수 / 2004. 11. 19. 채택)

Fracture-mechanical Modeling of Tool Wear by Finite Element Analysis

Ukhwan Sur† · Yeongseop Lee*
School of Mechanical & Automotive Engineering, Halla University
*Graduate School of Kangwon National University
(Received March 2, 2004 / Accepted November 19, 2004)

Abstract : Wear mechanisms may be briefly classified by mechanical, chemical and thermal wear. A plane strain finite element method is used with a new material stress and temperature fields to simulate orthogonal machining with continuous chip formation. Deformation of the workpiece material is treated as elastic-viscoplastic with isotropic strain hardening, and the numerical solution accounts for coupling between plastic deformation and the temperature field, including treatment of temperature-dependent material properties. Effects of the uncertainty in the constitutive model on the distributions of strain, stress and temperature around the shear zone are presented, and the model is validated by comparing average values of the predicted stress, strain, and temperature at the shear zone with experimental results.

초 록 : 마모구조는 대략적으로 기계, 화학 및 열적 마모 등으로 구분되어 진다. 평면변형 유한요소법이 지속적인 칩 형성을 갖는 대각선 가공을 시뮬레이션하기 위하여 새로운 재료의 응력 및 온도 필드와 같이 사용되었다. 작업소재의 변형은 등방성 변형 경화를 갖는 탄성-점소성으로 취급되며, 수치해석의 해는 소성 변형과 온도 필드의 결합을 설명하며, 온도 종속적인 재료 물성치로 취급된다. 이 논문에서 개발된 모델에서는 전단영역 주위의 변형률, 응력 및 온도 분포에 대한 구성모델의 불확실성의 영향들을 보여주며 예측된 전단영역의 응력, 변형률 및 온도의 평균값들은 기존의 실험 치와 비교해서 잘 맞는 것으로 사료된다.
Key Words : finite element modeling, machining simulations, orthogonal machining, thermo-mechanical modeling

1. Introduction

The prediction of wear of machine tools requires us to find the temperature fields during machining. Reference[1] is a discussion of tool wear due to dissolution and adhesion, and reference[2] is a discussion of wear of machine tools via dissolution[3] and abrasion[4]. These mechanisms are intimately related to the temperature of cutting.

Orthogonal turning is used as a standard for the study of the mechanisms of wear and tool failure.

Among machining process, orthogonal turning offers one of the most convenient setups for experimental measurements of strains, strain rates, and temperatures, and its two-dimensional mature makes it easier to model.

Although thermocouples and pyrometers are available to measure average temperatures and temperature fields near the cutting edge, there are as yet no models that are capable of predicting these experimental observations using material properties alone. This can be attributed to the complex, viscoplastic behavior of the workmaterial, the scarcity of information about the friction at the tool-chip and tool-flank interfaces, and the difficulty in accounting for the evolution in the extent of the tool-chip and tool-flank interfaces.

†To whom correspondence should be addressed.
uhsur@hit.halla.ac.kr

The formula

$$mc\Delta T = \Delta E \tag{1}$$

where m is the mass, c is the specific heat, ΔT is the change in temperature, and ΔE is the change in energy, can be used to get a rough approximation of the machining temperatures. In particular,

$$\Delta T = \frac{\Delta E}{mc} = \frac{Fv\Delta t}{(\rho A\Delta x)c} \tag{2}$$

where F is the cutting force, v is the cutting speed, ρ is the density, A is the area of contact at the tool-chip interface, and Δt and Δx are typical time and length scales. For the orthogonal turning of cast aluminum (319-T6) that has been done by us and using our numbers into equation (2) gives $\Delta T \approx 4000$ ℃, which far exceeds the usually observed values around 300 to 400℃.

The main fault of the above calculation is the assumption that all of the input power goes into heating the chip. The papers[5,6,7] discuss the modification of equation (2) using a heat partition β:

$$\Delta T_{xp} = \frac{\Delta E_{xp}}{mc} = \frac{\beta Fv\Delta t}{(\rho A\Delta x)c} \tag{3}$$

The use of heat partition, among other corrections, brings the temperature fields to values matching those of experiments. However, the main drawback to this approach is the reliance on the classical model of machining, which treats the primary and secondary shear zones as 2D planes. For a work-hardening material, the deformation zones flare out into 3D regions. This is discussed by Oxley[8], who arrives at analytical solutions by combining experimentally determined velocity fields with a generalization of the slip-line method to account for gardening. However, this approach is quite involved, especially in the case of complicated geometries.

In this paper, we are attempting to apply history-dependent constitutive equations to finite element models to get reliable temperature fields by the fracture mechanical approach. Knowledge of the temperature fields will be used to generalized the techniques of[2] to study the local evolution of tool wear, using a local convection-diffusion equation of transport. Estimations of the temperature fields using methods of[5-7], as well as the machining calculations of[8], will be used as benchmarks for the current approach. Our preliminary efforts using the FEM software ABAQUS follows closely the approach discussed in other researchers.

2. Finite element modeling

2.1. Finite element mesh

The initial workpiece mesh is shown in Fig. 1, where two-dimensional behavior is based on assuming a plane strain condition. The assumption is appropriate if the width of the cut, b, is much larger than the uncut chip thickness. The workpiece is represented by four node bilinear displacement and temperature plane strain elements, and since the objective is to obtain a steady-state solution, initial chip formation is prescribed to facilitate the analysis. Elements located along the tool-chip interface and the machined surface are refined to account for large deformation gradients.

A reference node which has both translational and rotational freedom is assigned to the rigid tool and acts as the master node for the tool. The motion of the rigid tool is entirely determined by the reference node, which can therefore be used to prescribe loads and kinematic constraints.

2.2. Modeling of workpiece-chip separation and tool-chip contact by fracture mechanical approach

A schematic showing the potential tool-chip and chip-workpiece surfaces is given in Fig. 1. Surface EF

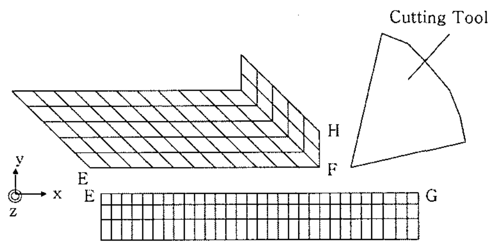

Fig. 1. Contact modeling

represents the bottom side of the potential chip, with its outward normal pointing downward, while surface EG represents the upper side of the machined surface, with its outward normal pointing upward. The two surfaces form a contact pair, with EF and EG providing master and slave surfaces, respectively. By definition, the nodes of the slave surface are constrained from penetrating into the master surface. Initially, the corresponding nodes on EF and EG are perfectly bonded and therefore have identical displacements in both x and y directions, as well as equivalent temperatures. During the simulation, the nodes debond to form a chip surface and a machined surface. This separation process is governed by a debonding direction specified in the model.

Although various chip separation criteria have been used in applying finite element analysis to metal cutting, a criterion based on controlled crack propagation is considered to be appropriate for this study, since material is ultimately separated through microcracks which develop as the tool moves onto the workpiece. Crack propagation through the material is illustrated schematically in Fig. 2. Selection of a crack length versus time relationship is based on movement of the cutting tool, and a reference point is defined on the slave surface, which is the machined surface from which crack length is measured. The length is calculated between the reference point and each node on the contact surfaces that may debond. Based on these lengths and the given crack length-time curve, the time increment is adjusted so that the debonding event occurs within the prescribed time tolerance for the crack to reach that length. The master and slave surfaces of the tool-chip contact pair consist of the rigid tool surface and surface EFH.

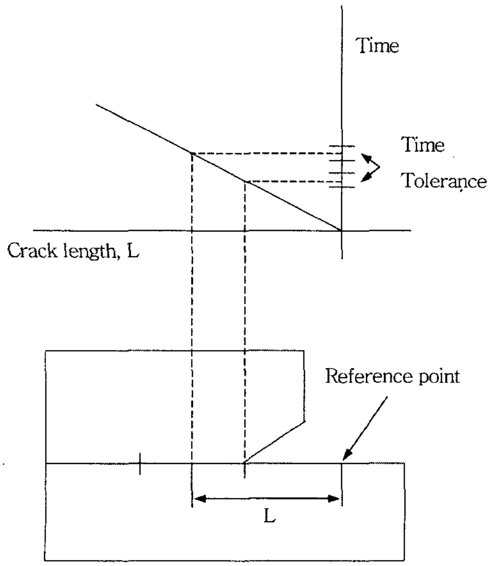

Fig. 2. Schematic for debonding of contact surface.

2.3. Boundary conditions

Kinematic boundary conditions (Fig. 3) are prescribed by constraining the left (AEL), right (BG) and bottom (AB) sides of the workpiece from any movement, while allowing all other boundaries to move. These conditions are valid as long as side AEL is far from the deformation zone and depth penetration on the machined surface is small. The cutting speed, U, is assigned to the cutting tool by choosing the time interval and corresponding tool displacement in the analysis. In this study, friction forces at the tool-chip interface are neglected, but a heat flux associate with friction effects is calculated from the machining experiments and applied to the contact area (Fig. 4). The secondary shear zone at the tool-chip interface is neglected, since it is localized within a very thin layer of the chip bottom and temperature distributions are of primary concern.

As shown in Fig. 4, the tip surface of the workpiece and exposed surfaces of the chip are assumed to be adiabatic ($\partial T/\partial n = 0$), since they are in contact with air, to which heat transfer may be neglected. The same assumption is made for the top and right boundaries of the machined workpiece material. The left and bottom

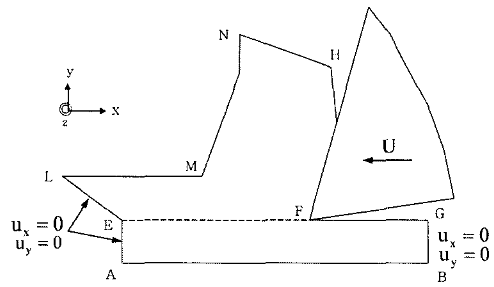

Fig. 3. Kinematic boundary conditions

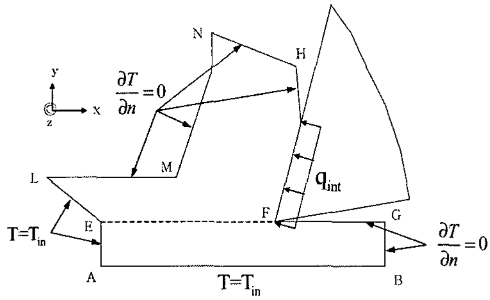

Fig. 4. Thermal boundary conditions.

boundaries of the workpiece are assumed to remain at the initial (room) temperature, since they are well removed from the deformation zone. Finally, a uniform heat flux is applied to the chip at the tool-chip interface to account for heat generation due to friction.

3. Finite element formulation

The general purpose finite element package ABAQUS^{TM} is used in this study to simulate the orthogonal machining process with a compatible displacement formulation.

4. Simulation of orthogonal metal cutting

A nonlinear temperature-displacement solution procedure is used to determine the coupled temperature and stress fields in the workpiece and the chip during material removal. Heat generation during plastic deformation may be expressed as

$$\dot{q}^{pl} = \eta \sigma \cdot \dot{\varepsilon}^{pl} \tag{4}$$

where $\dot{q}^{pl}$ is the volumetric rate of heat generation, η is the fraction of the mechanical work required for plastic deformation which is converted into thermal energy, σ is the stress, and $\dot{\varepsilon}^{pl}$ is the rate of plastic straining.

The steady-state, two-dimensional form of the energy equation governing the orthogonal machining process is

$$k\left(\frac{\partial^2 T}{\partial x^2}+\frac{\partial^2 T}{\partial y^2}\right)-\rho C_p\left(\partial\frac{T}{\partial}x+u_y\partial\frac{T}{\partial}y\right)+\dot{q}^{pl}=0 \tag{5}$$

where k is thermal conductivity, W/m/°C.

The temperatures are integrated using a backward difference scheme, and the coupled system is solved using Newton's method.

Nonlinearities in the numerical model are associated with material behavior, the geometry of the elements, and the change in boundary contact conditions. To enhance convergence, minimum and maximum time increments are specified, and within these limits actual increments are automatically adjusted based on the difficulty or ease with which convergence is achieved.

5. FEM simulation results

5.1. Simulation results

Each simulation starts as the tool moves towards the workpiece at a specified speed. The chip separates from the workpiece as debonding occurs at the contact surfaces and establishes contact with the tool rake face. To avoid instability of the numerical analysis caused by unbalanced forces at the nodes of the separating surfaces, a force reduction curve is specified to allow the forces to gradually reduce to zero.

From Fig. 5, which shows the strain distribution, it is evident that deformation begins ahead of the shear zone, and strain increases as the material moves towards the shear zone, until it reaches the upper boundary of the zone.

Stress distributions, which result from the combined effect of strain, strain rate and temperature, are shown in Fig. 6. When material moves towards central portions of the shear zone, the stress increases due to strain hardening and an increasing strain rate, until it

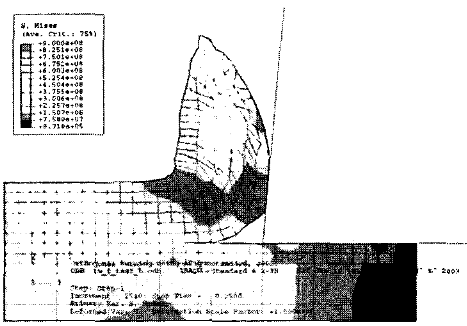
Fig. 5. Strain distribution

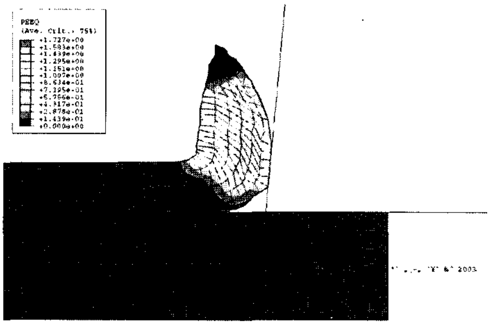

Fig. 6. Stress distribution.

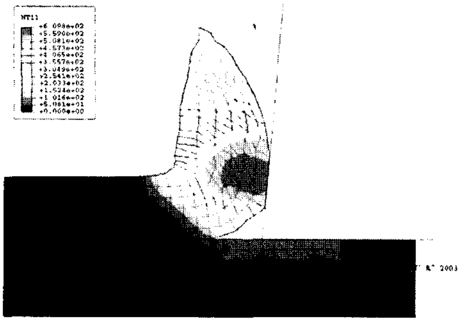

Fig. 7. Temperature distribution.

reaches a maximum at the center of the shear zone. The stresses are nearly uniform along the central shear zone, with lower values at the tool-chip interface where elevated temperatures act to soften the material. The temperature field is shown in Fig. 7. Temperatures increase due to plastic deformation in the material, as well as friction at the tool-chip interface. A high rate of deformation leads to concentrated heating of material in the deformation zone, with little heat transfer occurring by conduction from the zone. Temperatures begin to increase from the start of straining and continue to increase until straining ceases in the chip. However, temperature in a thin layer of material adjacent to the tool rake face also increases due to heat generated by friction.

Table 1. Comparison between experimental and simulation results along the central shear zone.

Case	Method	Temperature (°C)	Strain	Stress (MPa)
1	Machining test[2]	620	0.93	900
1	Simulation	590	1.04	910

One case was simulated to study the effects of cutting speed and preheating, and average values of stresses, strains and temperatures along the central shear zone are listed in Table 1.

6. Conclusions

A plane strain finite element simulation of an orthogonal machining process has been conducted, for which temperature and stress calculations are coupled with temperature-dependent material properties. The effects of strain hardening, strain rate, and temperature are considered by using a new material constitutive model developed for 1020 steel[9]. Parametric calculations to determine the effect of uncertainties in the constitutive model reveal a significant influence on the stress and temperature distributions.

Although the effect of frictional heating along the tool-chip interface is considered, the phenomenon has little effect on conditions in the primary shear zone. Distributions of strain, stress and temperature along the shear zone are presented for machining conditions corresponding to those considered experimentally, and the corresponding average values are in good agreement with those obtained from the measurement. Furthermore, we can apply history-dependent constitutive equations to finite element models to get reliable temperature fields. In addition to this, we can apply a fracture mechanical behaviors for tool wear.

Reference

1) E. Kannatey-Asibu Jr., "A Transport-Diffusion Equation in Metal Cutting and its Application to Analysis of the Rate of Flank Wear", Journal of Engineering for Industry-Transactions of the ASME, 107, pp. 81~89, 1985.
2) W.-S. Kim, T. P. K. Wong, and P. Kwon, "A Model-Based Prediction of Tool Wear", ASME Winter Annual Meeting, New York, NY, 2001.
3) B. M. Kramer, and N. P. Suh, "Tool Wear by Solution: A Quantitative Understanding", Journal of Engineering for Industry-Transactions of the ASME, 102, pp. 303~309, 1980.

4) E. Rabinowicz, "Abrasive Wear Resistance as a Materials Test", Lubrication Engineering, 33, pp. 378 ~381, 1977.
5) B. T. Chao, and K. J. Trigger, "Temperature Distribution at the Tool-Chip Interface in Metal Cutting", Transactions of the ASME, 77, pp. 1107~1119, 1955.
6) R. Komanduri, and Z. B. Hou, "Tribology in Metal Cutting-some Thermal Issues", Journal of Tribology-Transactions of the ASME, 123, pp. 799~815, 2001.
7) E. G. Loewen and M. C. Shaw, "On the analysis of Cutting-Tool Temperatures", Transactions of the ASME, 76, pp. 217~225(Discussion pp. 225-231), 1954.
8) P. L. B. Oxley, "Mechanics of Machining. An Analytical Approach to Assessing Machinability", Ellis Horwood Ltd., Chichester, 1989.
9) S. Lei, Y. C., Shin, F. P. Incropera, "Material constitutive modeling under high strain rates and temperatures through orthogonal machining tests", Proceedings of Manufacturing Science and Engineering, ASME IMECE, MEDvol. 6-2, 91~98, 1997.